Available online at www.sciencedirect.com
ScienceDirect
Ceramics International 34 (2008) 447–453
CERAMICS INTERNATIONAL
www.elsevier.com/locate/ceramint

Cobalt doped glass for the fabrication of percolated glass–alumina functionally graded materials

V. Cannillo [a], D. Mazza [b], C. Siligardi [a], A. Sola [a,*]

[a] *Dipartimento di Ingegneria dei Materiali e dell'Ambiente, Università di Modena e Reggio Emilia, Via Vignolese 905, 41100 Modena, Italy*
[b] *Dipartimento di Scienza dei Materiali ed Ingegneria Chimica, Politecnico di Torino, Italy*

Received 24 July 2006; received in revised form 16 September 2006; accepted 28 October 2006
Available online 18 December 2006

Abstract

The present research was focused on the development of a new glass to produce glass–alumina FGMs. The glass formulation, belonging to the $CaO–ZrO_2–SiO_2$ system, was doped with cobalt, by adding a small molar percentage (about 0.1 mol%) of CoO, in order to obtain a blue glass, which could be useful to appreciate the final compositional gradient. The glass was accurately characterized, evaluating its thermal behaviour, its mechanical properties, and its attitude to crystallize during a thermal treatment. Subsequently, the glass was used to produce glass–alumina FGMs via percolation and the so obtained specimens were analysed in order to evaluate the effect of the glass infiltration. The possible development of new crystal phases, in particular, was tested via micro X-ray diffraction and the elastic properties gradient associated with the compositional gradient was measured via depth-sensing Vickers microindentation.

Keywords: Co-glass; Alumina; Microdiffraction; Instrumented microindentation; Functionally graded materials

1. Introduction

Functionally graded materials (FGMs) are special composite systems, whose ingredient materials are properly distributed in space in order to create a compositional and/or microstructural gradient [1,2]. The related variation in thermo-mechanical properties, therefore, can be tailored to the prescribed loading conditions, while the smooth transition from one constituent phase to the other one avoids abrupt bi-materials joints, which can be detrimental to the reliability of multi-component systems [1–3]. Originally introduced as thermal barrier coatings in high-performance aerospace vehicles [4], FGMs have been promptly applied in several fields and nowadays they are commonly used not only as thermal barrier coatings (such as in turbines and high temperature engines [5,6]), but also as coatings to protect tools and mechanical devices against wear and erosion [7–9]. Moreover recent applications include biomaterials [10] and electronics [11] as well.

In the past, FGMs usually combined a ceramic phase and a metal one (this is the case, for example, of the aforementioned thermal barrier coating for aerospace vehicles) [12,13]; nevertheless also ceramic–ceramic and glass–ceramic FGMs have lately been widely studied, since they may show really interesting properties. In glass–alumina FGMs, for example, the optimisation of the elastic property gradient may result in a significant improvement of the resistance to hertzian cracking [14] and sliding contact damage [15] with respect to traditional composite materials and the bulk alumina itself. These promising glass–alumina systems, moreover, may be produced via percolation, which is a relatively easy method consisting in a thermal treatment, which induces the glass to melt and infiltrate into the polycrystalline alumina substrate [14,15]. The glass can be used both in powder form (suspension) and in bulk form, provided that it does not significantly interact with the alumina and it does not undergo relevant devetrification phenomena [16]. In fact, in spite of its apparent easiness, this technique requires an accurate selection of the ingredient materials in order to minimize the difference between their thermo-mechanical properties, which may induce residual stresses, and to reduce their potential interactions.

* Corresponding author. Tel.: +39 059 2056240; fax: +39 059 2056243.
E-mail address: sola.antonella@unimore.it (A. Sola).

0272-8842/$34.00
doi:10.1016/j.ceramint.2006.10.020

The present research was dedicated to the development of a new cobalt-doped glass, which could be applied to the production via percolation of glass–alumina FGMs. The original formulation, belonging to the ternary system CaO–ZrO_2–SiO_2 [17], was enriched with a small amount of cobalt (CoO at 0.1 mol%) in order to obtain a deep blue glass. In fact, the remarkably different colours of the constituent phases (alumina: white; glass: blue) could be helpful to check and appreciate the glass infiltration into the alumina substrate, which was visible even at the naked eye. The thermal behaviour as well as the thermo-mechanical properties of the glass were investigated in detail, in order to evaluate its suitability for the FGM production via percolation. Since the Co addition might enhance the glass devetrification, a particular attention was paid to the glass aptitude to crystallize during a thermal treatment and accurate tests were performed on both powder specimens and bulk specimens. Then some samples of glass–alumina FGMs were fabricated and observed by scanning electron microscopy (SEM). Several microdiffraction experiments were performed on the FGM cross section to check the possible development of new crystal phases caused by the heat treatment and the glass–alumina interaction. Moreover a systematic depth-sensing microindentation test was carried out on the FGM cross section, in order to evaluate the elastic property gradient.

2. Materials and methods

2.1. Glass

The glass formulation, reported in Table 1, was elaborated starting from the composition of a glass which, in the past, had been successfully used to produce glass alumina FGMs via percolation [17]. The glass was prepared using commercially available powder raw materials (quartz: Sikron 300 Colorobbia Italia; calcium carbonate: Colorobbia Italia; zirconium silicate: Zircobit FU, Colorobbia Italia; cobalt oxide Co_3O_4: Carlo Erba RPE, pure reagent grade), which were pre-mixed (by dry milling with alumina grinding bodies) and then melted in a platinum crucible. The heat treatment required to heat from room temperature to 500 °C at 5 °C/min and then from 500 to 1000 °C at 10 °C/min; an isothermal step of 60 min was performed at 1000 °C to allow the calcium carbonate to decompose; then the temperature was increased to 1500 °C at 10 °C/min and kept constant for 60 min to induce the complete melting of the glass. The melted glass was used to produce two types of samples: (i) bulk specimens were obtained by pouring the glass into moulds and then annealing them in a furnace at a temperature close to the glass transition temperature; (ii) some glass powder was produced by plunging the glass into cold water to obtain a frit which was wet ball milled and dried in a kiln. The granulometric distribution (Mastersizer, 2000 Ver. 5.22, Malvern Instruments Ltd.) of the powder was analysed.

Table 1
Glass molar composition

Oxide	mol%
CoO	0.10
CaO	39.74
ZrO_2	4.52
SiO_2	55.64

With respect to the original composition (CaO: 39.8 mol%; ZrO_2: 4.5 mol%; SiO_2: 55.7 mol% [17]), the glass was added a 0.1 mol% of CoO that was enough to give the glass a deep blue colour [18]. Though the introduced CoO amount was small, the presence of this additive could modify the thermal behaviour of the glass (glass transition temperature, softening point, crystallization aptitude, etc.) and its thermo-mechanical properties (elastic modulus, Poisson's ratio, toughness, coefficient of thermal expansion, etc.). Hence, an accurate investigation of the new glass was required.

First of all, the glass underwent a differential thermal analysis, DTA (NETZSCH, DSC 404), heating some powder from room temperature to 1400 °C at 10 °C/min. The thermal behaviour was further investigated with a heating microscope test (Expert System Solutions, Misura ODHT HSM 1600–80), heating a powder sample from room temperature to 1600 °C at 10 °C/min.

As shown in previous works [16], in the FGM production via percolation the glass can be used both in powder and in bulk form, but the uncontrolled sintering and/or crystallization of the glass should be avoided during the thermal treatment. Therefore the tendency of the Co-doped glass to sinter and/or to crystallize both in powder and in bulk form was investigated. As regards the behaviour of the glass in powder, it was studied by treating five powder specimens for 30 min at five different temperatures: 800, 900, 1000, 1100, and 1200 °C. In particular, the specimens were fabricated by humidifying the glass powder with water at 6 wt.% and then pressing it at 300 kg_f/cm^2 (28 MPa) thus obtaining disk shaped samples (diameter: 40 mm; thickness: 4 mm); the disks were cut into four quarters, each of which was heat treated at a different temperature. The same thermal treatments were repeated on five bulk samples (4 mm × 4 mm × 5 mm). Then all the resulting samples (five obtained starting from glass powder and five obtained starting from glass bulks) were ground and tested via X-ray diffraction, XRD (Philips PW 3710). The coefficient of thermal expansion was measured with a NETSCH, DIL 404 dilatometer, heating a glass bar (4 mm × 4 mm × 50 mm) from room temperature to the dilatometric softening point at 10 °C/min. The elastic properties of the glass were measured with a resonance based technique (EMOD, Lemmens Grindosonic® MK5) on a bulk disk-shaped (diameter: 50 mm; thickness: 5 mm) sample. Moreover, in order to evaluate the glass hardness and toughness, a Vickers microindentation test (REMET HX-1000) was performed on a bulk sample previously embedded in resin and carefully polished. A maximum load of 100 g_f was applied for 15 s to determine the glass hardness (by measuring the indent diagonal length [19] during a SEM observation, PHILIPS XL 40); then the maximum load was increased to 300 g_f to estimate the glass toughness (by measuring the crack length [20]).

2.2. Functionally graded materials

As regards the glass–alumina FGM fabrication, a commercial sintered alumina was chosen (Kéramo ceramiche tecniche, Tavernerio (CO), Italy). The alumina, which was a high purity (99.7%) product supplied in form of tiles, was observed with SEM and its residual porosity was quantified via an image elaboration analysis. The alumina mineralogical composition was identified by a XRD test and its coefficient of thermal expansion was measured following the same method applied to the glass (maximum temperature reached: 1400 °C). The elastic properties, Vickers hardness and toughness of the alumina were determined as well.

Due to the thermal behaviour of the glass, as described in the next paragraph, the FGM production was carried out starting from the glass in bulk form and not in powder form: a thin flat piece of glass was placed on the top surface of an alumina tile and heat treated for four hours at 1600 °C. As a consequence, the glass melted and percolated into the alumina substrate [14,21]. The resulting samples were cut and polished; then, the cross section was observed with SEM. Due to the potential aptitude of the glass to crystallize, the effect of the thermal treatment and glass percolation on the mineralogical composition of the system was to be evaluated in detail. With this aim, a X-ray microdiffraction was performed on the FGM cross section mounting a 300 μm collimator in order to focus the X-ray beam. The equipment (Rigaku D-max microdiffractometer) employs an Image Plate 2600 × 4600 pixel wide with 10^6 linear response, thus allowing fast collection rates (around 20 min) in a wide solid angle. Several images were collected along the glass penetration direction: the test points were equally spaced, with a distance of about 500 μm, and the first test point was placed at about 700 μm of depth. In order to establish a benchmark, an image was collected on the pure alumina cross section under the same experimental conditions. All the images were analyzed with Rigaku sofware and transformed in 2θ-intensity patterns.

To conclude, the functional gradient associated with the spatial change in composition and microstructure of the FGM was evaluated through a systematic Vickers microindentation test on the FGM cross section (applied load: 500 g_f); a depth-sensing technique (OpenPlatform, C.S.M. Instruments) was adopted to measure the local elastic modulus of the material and define the variation of the elastic properties occurring along the glass percolation direction [22]. The evaluation was performed up to 1500 μm of depth, since several technical and engineering applications involve the surface and sub-surface properties of the system (e.g. hertzian contact, abrasion resistance, erosion resistance, etc.).

3. Results and discussion

3.1. Glass

3.1.1. Glass in powder form

Though the granulometric distribution exhibited a bi-modal trend, the glass powder was on average very fine, with D50 at about 10 μm and D90 at about 32 μm, as shown in Fig. 1.

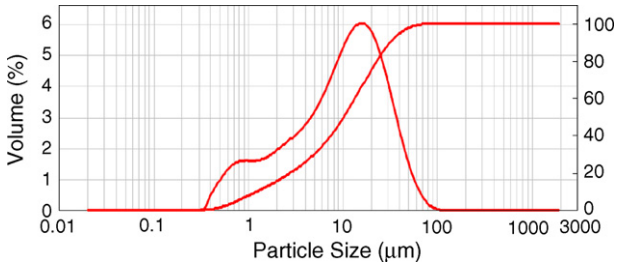

Fig. 1. Particle size distribution of the glass powder.

The DTA of the glass (performed on the glass powder, as already said), which is reported in Fig. 2, revealed that the glass transition occurred at about 750 °C; the exothermal peak at about 950 °C was likely to be associated with the crystallization of the glass, while the weak endothermal peak at about 1150 °C was probably caused by a polymorphous transformation of the newly formed crystal phase [17,23]. Both the glass transition temperature and the crystallization temperature were slightly reduced by the cobalt introduction with respect to the initial $CaO–ZrO_2–SiO_2$ formulation [17], since the cobalt behaved as a glass-modifier. Moreover, as regards the thermal behaviour of the glass, it was possible to identify the sintering point (about 880 °C), the softening point (about 894 °C) and the melting point (about 1420 °C). The sphere point and the half sphere point could not be determined, since the glass sample, after sintering, substantially kept its shape until it quickly melted. These results suggest that the glass first sintered (at about 880 °C) and then crystallized (at about 950 °C); then, the newly developed crystal phase underwent a polymorphous transformation (at about 1150 °C), a process which was detected by the DTA but not by the heating microscope; in the end, the system melted (at about 1420 °C).

These considerations were confirmed by the sintering/crystallization tests performed on the glass powder disks, whose results are summarized in Table 2. In fact, if the temperature of the heat treatment was lower than 950 °C, the samples sintered but remained substantially amorphous; on the contrary, if the temperature exceeded 950 °C, a wide crystallization of wollastonite occurred (as proved by the XRD). In particular, if the specimens were heat treated at 1000 or 1100 °C, the 2M-wollastonite (JCPDS-ICDD 27–88) could be identified but, if the maximum temperature was 1200 °C, the

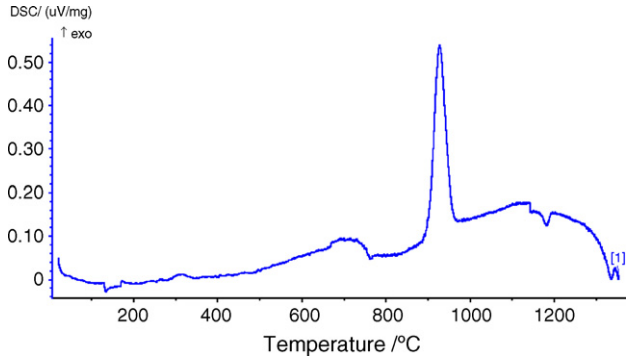

Fig. 2. DTA of the glass.

Table 2
Effects of the thermal treatments on powder glass samples

Temperature (°C)	Main effect of heating	Crystal phases identified
800	Sintering	–
900	Sintering	–
1000	Crystallization	2M-wollastonite
1100	Crystallization	2M-wollastonite
1200	Crystallization	Cyclo-wollastonite

2M-wollastonite was replaced by the pseudo-wollastonite (JCPDS-ICDD 31-300). In fact, the 2M-wollastonite becomes thermodynamically unstable at about 1125 °C and it tends to transform in pseudo-wollastonite; this transformation may justify the aforementioned endothermal peak in the DTA graph. The diffraction patterns referring to the glass powder samples are shown in Fig. 3; for clarity reasons, in this picture the spectra were progressively shifted along the ordinate axis.

3.1.2. Glass in bulk form

On the contrary, it is really worth noting that the heat treatments did not induce any relevant sintering and/or crystallization of the bulk glass samples, which remained amorphous as shown in Fig. 4: this picture represents the diffraction pattern of the sample heat treated at the highest temperature (1200 °C), but all the spectra, independently of the

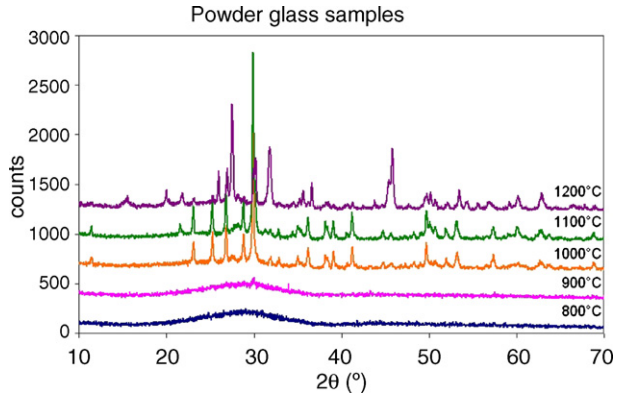

Fig. 3. XRD patterns of the samples produced starting from the glass powder.

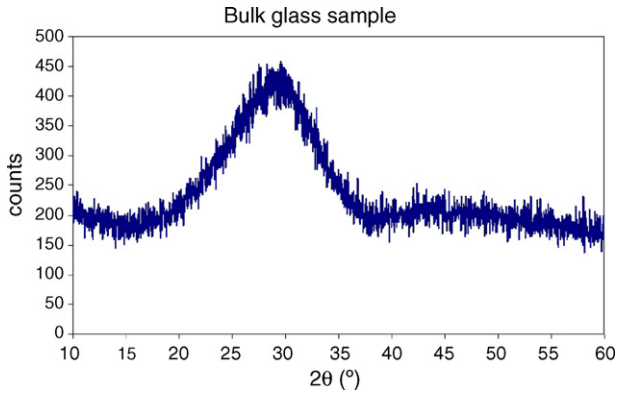

Fig. 4. Example of the XRD patterns of the samples produced starting from the glass bulks (specimen heat treated at 1200 °C).

temperature, were substantially analogous. It can be deduced that the crystallization kinetics were significantly reduced for the bulk specimens which, therefore, were not modified by the thermal treatment.

Actually, as already proved in previous works [17,23], the glasses belonging to the ternary system CZS (without cobalt) preferentially undergo a surface crystallization. When they are heat treated in powder form, they usually sinter at about 850 °C and then crystallize at 1050 °C, with the development of wollastonite as main phase and, in case, calcium zirconium silicate ($Ca_2ZrSi_4O_{12}$) as secondary phase; fluctuations of the sintering and crystallization temperatures can be observed according to the specific formulation considered. Therefore it seems that the cobalt introduction into the glass composition slightly reduced the characteristic temperatures of the glass; moreover, the cobalt could promote the crystallization of the crystal phase 2M-wollastonite while reducing the genesis of calcium zirconium silicate.

The dilatometric test proved that the coefficient of thermal expansion (calculated from room temperature to the glass transition temperature) was $9.2 \times 10^{-6}\,K^{-1}$. This value was still comparable with that of the starting CZS glass ($8.7 \times 10^{-6}\,K^{-1}$) [17], but the small increase in the coefficient of thermal expansion confirmed that the cobalt acted as a modifier in the glass formulation.

As regards the mechanical properties of the glass, the Young's modulus resulted to be 96.6 GPa and the Poisson's coefficient 0.30; the indentations at 100 g_f gave $HV_{100} = 9.0 \pm 0.7$ GPa and those at 300 g_f allowed to evaluate $K_{IC} = 0.52 \pm 0.06$ MPa $m^{1/2}$ (this value was deduced by the length of the cracks at the indent tips). These values, which were comparable with those of the original CZS glass, were relatively good for a glass. Presumably the presence of ZrO_2 in the glass formulation improved the mechanical properties of the glass, which were not altered by the addition of CoO.

It appears reasonable to conclude that the addition of 0.1 mol% CoO was enough to confer the glass a dark blue colour and weakly modify the thermal behaviour of the glass, but not enough to relevantly change its main mechanical properties (such as Young's modulus and hardness). The new Co-doped glass, therefore, was a promising candidate for the FGM production via percolation, since the difference in colour between the constituent phases could make evident (even at the naked eye) the glass infiltration into the alumina substrate. However, in order to produce the FGM via percolation, the glass was employed only in bulk, while the powder was disregarded due to its uncontrolled aptitude to crystallize.

3.2. Functionally graded materials

The alumina, which was used as a substrate in the FGM production, was a polycrystalline material with a residual porosity of about 5.6 ± 0.7 vol.%; this value was deduced by the image elaboration of 10 micrographs. As represented in Fig. 5, the XRD pattern proved the existence of only one crystal phase, i.e. α-alumina (corundum). The coefficient of thermal expansion of the alumina, calculated from room temperature to

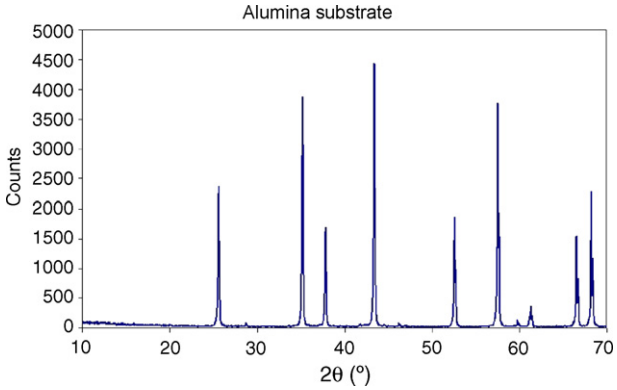

Fig. 5. XRD pattern of the alumina used as substrate in the FGM production.

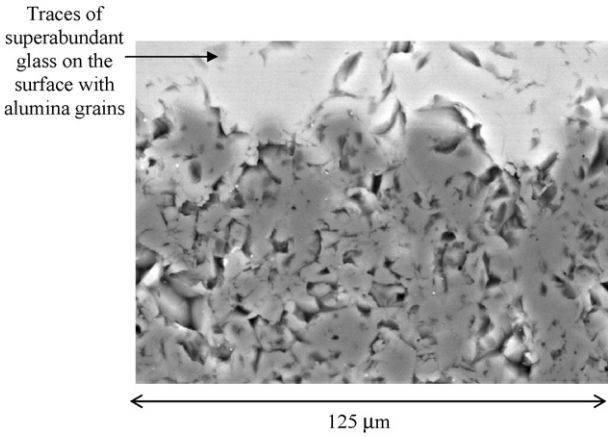

Fig. 7. SEM image of the FGM cross section.

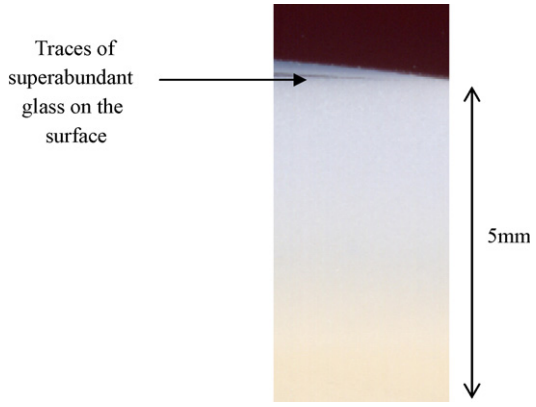

Fig. 6. Photograph of a portion of the FGM cross section.

the glass transition temperature, was $8.3 \times 10^{-6}\,K^{-1}$. This value was lower than the glass one, suggesting that in the final FGM the alumina would result slightly in compression and the glass in traction. However it was likely that the difference was not great enough to compromise the FGM production [24]. The mechanical properties of the alumina were really good, with a Young's modulus equal to 379.2 GPa, a Poisson's coefficient equal to 0.21, a Vickers hardness $HV_{500} = 20.9 \pm 2.0$ GPa and a fracture toughness $K_{IC} = 4$ MPa $m^{1/2}$.

Fig. 6 reproduces a photograph of a part of the FGM cross section. Thanks to the deep blue colour of the Co-doped glass, the infiltration of the glass into the polycrystalline alumina could be visually appreciated. In fact the gradual change in colour of the FGM cross section, from blue to white, was the result of the smooth variation in the relative amounts of glass and alumina along the percolation direction. The investigation by sight of the cross section suggested that the glass could infiltrate very deeply into the alumina bulk, reaching a depth of about 4 mm. This qualitative evaluation was confirmed by the X-EDS measurements on the FGM cross section, which allowed to detect some Si down to about 4.5 mm of depth (since the substrate was made of alumina, the Si could be considered as a marker of the glass). The infiltration was also confirmed by the SEM investigation of the cross section, which showed the presence of glass along the alumina grain boundaries and inside pores. Moreover the SEM inspection suggested that some superficial alumina grains could diffuse into the (residual)

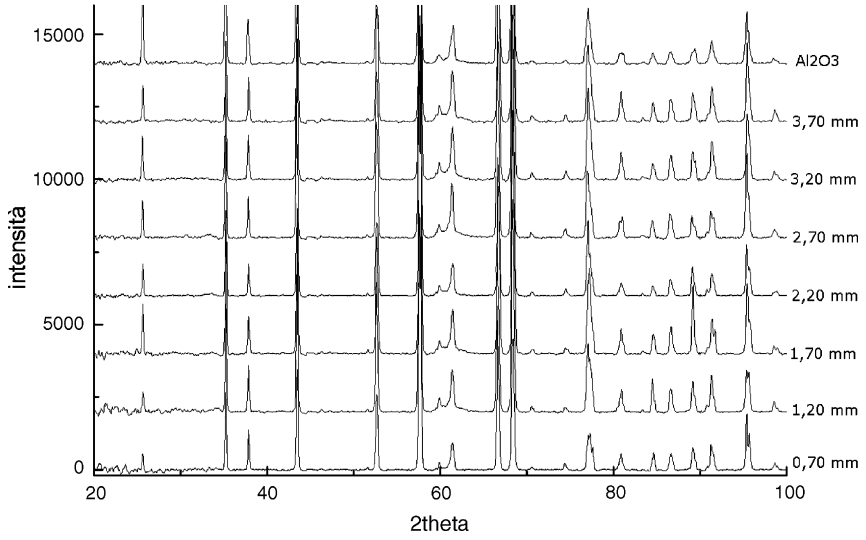

Fig. 8. Comparison between the micro-diffraction patterns collected on the FGM cross section at increasing depths and the pattern of the pure alumina.

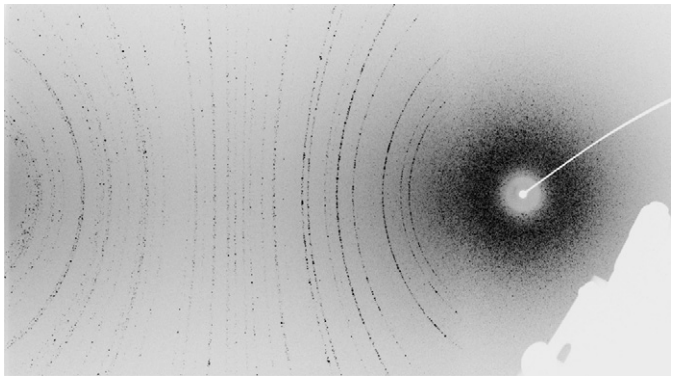

Fig. 9. Image as collected from the image plate of the diffractometer while analysing the pure alumina.

superabundant glass, which remained on the top surface of the FGM, as shown in Fig. 7.

In order to check the effect of the thermal treatment and glass percolation on the crystal composition of the resultant FGM, a micro-diffraction test was required. The spectra were collected on the graded area of the cross section in order to cut off as much as possible the portion of the alumina substrate, which had not been involved in the glass percolation. As reported in Fig. 8, the patterns, which referred to different depths along the infiltration direction, were all dominated by the alumina peaks (α-alumina, ICDD 42-1468) and it was not possible to identify relevant peaks associated with other crystal phases. At most, some variations in the peak shape occurred in the intervals $2\theta = 70–80^\circ$ and $90–100^\circ$. However, no other relevant changes could be detected with respect to the pure alumina pattern and therefore it is reasonable to exclude significant crystallizations of new phases. Fig. 9 represents an image as extracted from the image plate of the micro-diffractometer; the measure time was 20 min and the test was performed on the first point on the cross section, at about 700 μm of depth.

The depth sensing micro-indentation test, whose results are reported in Fig. 10, proved that the compositional variation along the percolation direction actually resulted in a functional gradient, since the local elastic modulus progressively increased with increasing alumina contents. When the system is loaded (for example, during a Hertzian contact), a proper variation in the elastic modulus along the infiltration direction may cause a stress redistribution, resulting in improved surface performances [14].

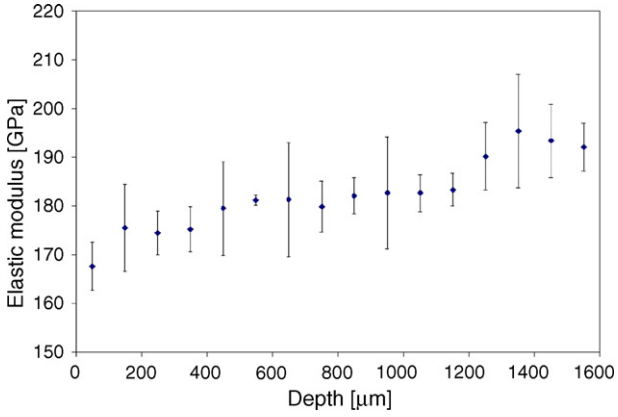

Fig. 10. Local elastic modulus as a function of depth in FGMs.

4. Conclusions

In the past, cobalt blue glasses have been widely used to fabricate artistic windows, bottles, cosmetic containers and other fine objects. Cobalt blue glasses, moreover, have been applied to produce optical filters (for example, in the flame test) and glazings with a reduced energy transmittance. In the present work, a Co-doped glass was prepared and investigated in view of its application in the fabrication of glass–alumina functionally graded materials. The experimental tests proved that the cobalt-doped glass had really interesting thermo-mechanical properties, such as a high elastic modulus, a good fracture toughness and a coefficient of thermal expansion fairly similar to the alumina one. Due to the aptitude of the glass in powder form to sinter and crystallize during a heat treatment, the functionally graded material samples were fabricated starting from glass bulks (slices). Since the ingredient materials had completely different colours – white the alumina and deep blue the glass – it was possible to appreciate immediately the glass infiltration into the alumina substrate, made evident by the gradual change in colour on the FGM cross section. However the glass percolation was also experimentally confirmed by the SEM-EDS investigation. To conclude, a detailed micro-diffraction test on the FGM cross section revealed that the heat treatment and the glass percolation did not cause relevant crystallizations of new phases. The cobalt-doped glass, therefore, could be successfully used to produce new glass–alumina functionally graded materials, in which the different colours of the constituent phases was helpful to verify the glass infiltration and appreciate the compositional gradient.

References

[1] A. Kawasaki, R. Watanabe, Concept and P/M fabrication of functionally graded materials, Ceram. Int. 23 (1997) 73–83.
[2] Y. Miyamoto, W.A. Kaysser, B.H. Rabin, A. Kawasaki, R.G. Ford, Functionally graded materials, in: Design, Processing and Applications, Kluwer Academic Publishers, 1999.
[3] A. Kawasaki, R. Watanabe, Thermal fracture behavior of metal/ceramic functionally graded materials, Eng. Fract. Mech. 69 (14/16) (2002) 1713–1728.
[4] M. Koizumi, M. Niino, Overview of FGM research in Japan, MRS Bull. 1 (1995) 19–21.
[5] H. Cetinel, B. Uyulgan, C. Tekmen, I. Ozdemir, E. Celik, Wear properties of functionally gradient layers on stainless steel substrates for high temperature applications, Surf. Coat. Technol. 174/175 (2003) 1089–1094.
[6] H. Hamatani, N. Shimoda, S. Kitaguchi, Effect of the composition profile and density of LPPS sprayed functionally graded coating on the thermal shock resistance, Sci. Technol. Adv. Mater. 4 (2) (2003) 197–203.
[7] U. Schulz, M. Peters, Fr.-W. Bach, G. Tegeder, Graded coatings for thermal, wear and corrosion barriers, Mater. Sci. Eng. A A362 (1/2) (2003) 61–80.

[8] L. Prchlik, S. Sampath, J. Gutleber, G. Bancke, A.W. Ruff, Friction and wear properties of WC-Co and Mo-Mo_2C based functionally graded materials, Wear 249 (12) (2001) 1103–1115.
[9] H.X. Zhao, M. Yamamoto, M. Matsumura, Slurry erosion properties of ceramic coatings and functionally gradient materials, Wear 186/187 (2) (1995) 473–479.
[10] R. Roop Kumar, M. Wang, Functionally graded bioactive coatings of hydroxyapatite-titanium oxide composite system, Mater. Lett. 55 (2002) 133–137.
[11] E. Müller, Č Drašar, J. Schilz, W.A. Kaysser, Functionally graded materials for sensor and energy applications, Mater. Sci. Eng. A A362 (1/2) (2003) 17–39.
[12] A. Mortensen, S. Suresh, Functionally graded metals and metal-ceramic composites. I. Processing, Int. Mater. Rev. 40 (6) (1995) 239–265.
[13] A. Mortensen, S. Suresh, Functionally graded metals and metal-ceramic composites. II. Thermomechanical behaviour, Int. Mater. Rev. 42 (3) (1997) 85–116.
[14] J. Jitcharoen, N.P. Padture, A.E. Giannakopoulos, S. Suresh, Hertzian-crack suppression in ceramics with elastic-modulus-graded surfaces, J. Am. Ceram. Soc. 81 (9) (1998) 2301–2308.
[15] S. Suresh, M. Olsson, A.E. Giannakopoulos, N.P. Padture, J. Jitcharoen, Engineering the resistance to sliding-contact damage through controlled gradients in elastic properties at contact surfaces, Acta Mater. 47 (14) (1999) 3915–3926.
[16] V. Cannillo, T. Manfredini, C. Siligardi, A. Sola, Preparation and experimental characterization of glass–alumina functionally graded materials, J. Eur. Ceram. Soc. 26 (6) (2006) 993–1001.
[17] V. Cannillo, T. Manfredini, M. Montorsi, C. Siligardi, A. Sola, Glass–alumina functionally graded materials: their preparation and compositional profile evaluation, J. Eur. Ceram. Soc. 26 (13) (2006) 2685–2693.
[18] J.M.F. Navarro, El Vidrio, C.S.I.C., Madrid, 1991.
[19] G.D. Quinn, P.J. Patel, I. Lloyd, Effect of loading rate upon conventional ceramic microindentation hardness, J. Res. Natl. Inst. Std. Technol. 107 (3) (2002) 299–306.
[20] C.B. Ponton, R.D. Rawlings, Vickers indentation fracture test. Part 1. Review of literature formulation of standardised indentation toughness equations, Mater. Sci. Technol. 5 (1989) 865–871.
[21] P.L. Flaitz, J.A. Pask, Penetration of polycristalline alumina by glass at high temperatures, J. Am. Ceram. Soc. 70 (7) (1987) 449–455.
[22] W.C. Oliver, G.M. Pharr, An improved technique for determining hardness and elastic modulus using load and displacement sensing indentation experiments, J. Mater. Res. 7 (6) (1992) 1564–1583.
[23] C. Leonelli, C. Siligardi, CaO–SiO_2–ZrO_2 glasses: modelling and experimental approach, Recent Res. Develop. Mater. Sci. 3 (2002) 599–618.
[24] V. Cannillo, G. de Portu, L. Micele, M. Montorsi, G. Pezzotti, C. Siligardi, A. Sola, Microscale computational simulation and experimental measurement of thermal residual stresses in glass–alumina functionally graded materials, J. Eur. Ceram. Soc. 26 (8) (2006) 1411–1419.